

CR 114663
AVAILABLE TO THE
PUBLIC



National Research
Council Canada

Conseil national
de recherches Canada

(NASA-CR-114663)	SUPERSONIC EXPERIMENTS	N73-30944
ON DYNAMIC CROSS-DERIVATIVES DUE TO		
PITCHING AND YAWING OF AIRCRAFT-LIKE		
VEHICLES (National Research Council of		Unclas
Canada) 45 p HC \$4.25	CSCL 01C	G3/02 13783

NATIONAL AERONAUTICAL ESTABLISHMENT

LABORATORY TECHNICAL REPORT

LTR - UA - 24

SUPERSONIC EXPERIMENTS
ON DYNAMIC CROSS DERIVATIVES
DUE TO PITCHING AND YAWING
OF AIRCRAFT - LIKE VEHICLES

K. J. ORLIK - RÜCKEMANN, J. G. LABERGE AND E. S. HANFF

RAPPORT TECHNIQUE DE LABORATOIRE

ÉTABLISSEMENT AÉRONAUTIQUE NATIONAL

AUGUST 1973
OTTAWA, CANADA

NATIONAL AERONAUTICAL
ESTABLISHMENT



ÉTABLISSEMENT AÉRONAUTIQUE
NATIONAL

CANADA

PAGES 28
PAGES

FIG. 14
DIAG.

REPORT
RAPPORT

REPORT LTR-UA-24
RAPPORT

DATE AUGUST 1973
DATE

SECTION

LAB. ORDER NAE 1671 (R)
COMM. LAB.

UNSTEADY AERODYNAMICS LABORATORY

FILE 49-10N-5
DOSSIER

FOR NASA Ames Research Center
POUR

REFERENCE Contract NASW-2369; Contract Monitor - G. Malcolm
RÉFÉRENCE

LTR-UA-24

SUPERSONIC EXPERIMENTS
ON DYNAMIC CROSS-DERIVATIVES
DUE TO PITCHING AND YAWING
OF AIRCRAFT-LIKE VEHICLES

SUBMITTED BY K.J. Orlik-Rückemann
PRÉSENTÉ PAR
SECTION HEAD
CHEF DE SECTION

K.J. Orlik-Rückemann
J.G. LaBerge
AUTHOR E.S. Hanff
AUTEUR

APPROVED F.R. Thurston
APPROUVÉ
DIRECTOR
DIRECTEUR

LIST OF CONTENTS

	<u>Page</u>
Abstract	(i)
Symbols	(ii)
1. Introduction	1
2. Basic principles of apparatus	3
3. Mechanical arrangement	4
3.1 Design considerations	
3.2 Driving mechanism	
4. Instrumentation	6
5. Experimental procedures	5
5.1 Bench calibrations	
5.2 Calibrations in the wind tunnel	
5.3 Wind tunnel experiments	
6. Data reduction	10
6.1 General	
6.2 Direct derivatives	
6.3 Cross-derivatives	
7. Wind tunnel and model	15
8. Experimental program and results	15
8.1 Program	
8.2 Results	
8.3 Additional experiments on cones	
9. Summary and conclusions	19
10. Acknowledgement	20
11. References	21
Tables 1 - 2	
Figures 1 - 14	

ABSTRACT

A new wind tunnel apparatus has been developed and constructed for the determination of moment cross-derivatives due to pitching and yawing on models at moderate angles of attack and sideslip. The apparatus can also be used to determine the direct moment derivatives in pitch and yaw. Experimental results were obtained at Mach 2 on a cone-wing-fin configuration at angles of attack and sideslip up to 15° . Although at small values of these angles the cross-derivatives were always negligibly small, measurable effects were sometimes observed, at all angles of attack included in this investigation (i.e. up to 15°), when the angle of sideslip was 10° or 15° . For dynamic cross-derivatives $(C_{lq} + C_{l\dot{\alpha}})$, $(C_{mr} - C_{m\dot{\beta}} \cos \alpha_0)$ and $(C_{nq} + C_{n\dot{\alpha}})$ [which represent the coupling between the lateral and the longitudinal degrees of motion] these effects were of the order of up to 5 percent of the direct damping derivative in the pertinent equation of motion and can probably be expected to be even larger for higher values of angles of attack and sideslip and for configurations more prone to asymmetric vortex shedding (such as a winged configuration with a long forebody). If so, it may be desirable to include such derivatives in the flight mechanics analysis of aircraft flying at moderate angles of attack and sideslip, such as may be encountered during certain high performance maneuvers, when using direct lift or side-force control, or during certain phases of spin motion. To the best knowledge of the present authors, the three cross-derivatives in question have never been determined before.

SYMBOLS

All stability derivatives are referred to the body axis system.

A_b	base area of the model
c	$\cos\alpha_0$
C_ℓ	$M_x / (\bar{q}A_b \ell)$
C_m	$M_y / (\bar{q}A_b \ell)$
C_n	$M_z / (\bar{q}A_b \ell)$
I_y	moment of inertia around the pitch axis
k	angular stiffness
ℓ	model length
M	Mach number
M_x	rolling moment
M_y	pitching moment
M_z	yawing moment
p	angular velocity in roll
q	angular velocity in pitch
\bar{q}	dynamic pressure
r	angular velocity in yaw
t	time
V	freestream velocity
α	angle of attack; angular deflection in pitch
α_0	mean angle of attack
$\dot{\alpha}$	time rate of change of angle of attack
β	angle of sideslip
β_0	mean angle of sideslip
$\dot{\beta}$	time rate of change of angle of sideslip
Θ	angular deflection in pitch, $\Theta = \alpha$
μ	damping coefficient
ϕ	angular deflection in roll
ψ	angular deflection in yaw, $\Psi = -\beta$
ω	(circular) frequency

Subscripts:

Θ	refer to oscillation in pitch
ϕ	refer to oscillation in roll
Ψ	refer to oscillation in yaw
I	refer to model position for direct derivative measurement in the plane indicated
II	refer to model position for cross-derivative measurement in the plane indicated

Derivatives

$$C_{l\alpha} = \frac{\partial C_l}{\partial \alpha}$$

$$C_{m\alpha} = \frac{\partial C_m}{\partial \alpha}$$

$$C_n = \frac{\partial C_n}{\partial \alpha}$$

$$C_{l\beta} = \frac{\partial C_l}{\partial \beta}$$

$$C_{m\beta} = \frac{\partial C_m}{\partial \beta}$$

$$C_{n\beta} = \frac{\partial C_n}{\partial \beta}$$

$$C_{l\dot{\alpha}} = \frac{\partial C_l}{\partial \frac{\dot{\alpha} \ell}{2V}}$$

$$C_{m\dot{\alpha}} = \frac{\partial C_m}{\partial \frac{\dot{\alpha} \ell}{2V}}$$

$$C_{n\dot{\alpha}} = \frac{\partial C_n}{\partial \frac{\dot{\alpha} \ell}{2V}}$$

$$C_{l\dot{\beta}} = \frac{\partial C_l}{\partial \frac{\dot{\beta} \ell}{2V}}$$

$$C_{m\dot{\beta}} = \frac{\partial C_m}{\partial \frac{\dot{\beta} \ell}{2V}}$$

$$C_{n\dot{\beta}} = \frac{\partial C_n}{\partial \frac{\dot{\beta} \ell}{2V}}$$

$$C_{lq} = \frac{\partial C_l}{\partial \frac{q \ell}{2V}}$$

$$C_{mq} = \frac{\partial C_m}{\partial \frac{q \ell}{2V}}$$

$$C_{nq} = \frac{\partial C_n}{\partial \frac{q \ell}{2V}}$$

$$C_{lr} = \frac{\partial C_l}{\partial \frac{r \ell}{2V}}$$

$$C_{mr} = \frac{\partial C_m}{\partial \frac{r \ell}{2V}}$$

$$C_{nr} = \frac{\partial C_n}{\partial \frac{r \ell}{2V}}$$

Note: For oscillation around a fixed body axis at an angle of attack, α_0 , the dynamic derivatives appear in the following combinations:

$$C_{lq} + C_{l\dot{\alpha}}$$

$$C_{mq} + C_{m\dot{\alpha}}$$

$$C_{nq} + C_{n\dot{\alpha}}$$

$$C_{lr} - cC_{l\dot{\beta}}$$

$$C_{mr} - cC_{m\dot{\beta}}$$

$$C_{nr} - cC_{n\dot{\beta}}$$

where $c = \cos \alpha_0$.

1. INTRODUCTION

As shown by Tobak and Schiff in Reference 1, the nonlinear moment system for arbitrary motions of both axisymmetric and nonaxisymmetric bodies may be completely specified by moment contributions resulting from four characteristic simple motions. In a body-axis system, these four motions are: (a) steady flight, (b) coning motion, (c) oscillation in pitch, (d) oscillation in yaw - all of these at a combination of a constant angle of attack and angle of sideslip. For each of these motions the pitching, yawing and rolling moments are required. The moments associated with (a) can be obtained from static wind tunnel measurements, and the moments associated with (b) from measurements on a special coning apparatus such as the one described in Reference 2. The moments associated with (c) and (d) consist partly of pure damping-in-pitch and damping-in-yaw derivatives (and their static counterparts) which can be obtained from one-degree-of-freedom oscillatory experiments, and partly from static and dynamic cross-derivatives, such as yawing and rolling moments due to pitching, and pitching and rolling moments due to yawing.

Of the above dynamic cross-derivatives, the only one that has been considered in the past is the rolling moment due to yawing. The remaining three derivatives all represent a cross-coupling between the longitudinal and the lateral degrees of freedom and up to now have always been considered negligible. To the best knowledge of the present authors no attempt has ever been made to determine them either theoretically or experimentally. Of course, in the past there was no real need to know these

derivatives, since in most low angle-of-attack and low angle-of-sideslip flight conditions they were, in fact, extremely small if not zero. However, as discussed in References 3 and 4, with the present-day high performance maneuvers and the possible use of direct lift and side-force control, this situation has now changed. Separated flows and asymmetric vortex shedding, which occur at higher angles of attack and sideslip, are known to cause severe flow asymmetries, which in turn may introduce non-negligible cross-coupling derivatives.

Except for the forced oscillation apparatus in the Full Scale Tunnel at NASA Langley (with which many of the required cross-derivatives can be measured at Mach numbers up to 0.1) and the recently modified forced-oscillation apparatus (Reference 3) in the High Speed Aircraft Division at NASA Langley (with which it may be possible to measure the rolling moment due to yawing at Mach numbers from 0.2 to 4.6), no operational apparatus seems to exist at the present time with which any of the required cross-derivatives could be obtained in the wide range of Mach numbers which is of interest for present-day flight operations. It was the purpose of this project to develop and construct a pilot model of such an apparatus and to assess its sensitivity and accuracy by conducting a preliminary series of experiments on a simple model in a supersonic wind tunnel. This report gives a brief description of the apparatus and of the specially-developed instrumentation system, a discussion of the calibration and testing procedures, an account of the method for data reduction and analysis, and includes some experimental results obtained on a cone-wing-fin configuration at Mach 2 and at angles of attack and sideslip up to 15°.

2. BASIC PRINCIPLES OF APPARATUS

The apparatus provides a forcing oscillatory motion in pitch with resulting forced oscillatory motions in yaw and roll or, alternatively, with the model rotated 90° around its longitudinal axis, a forcing oscillatory motion in yaw with resulting forced oscillatory motions in pitch and roll. In each case the torque, the amplitude and the frequency of the forcing motion, as well as the in-phase and quadrature components of the two forced motions with respect to the forcing motion are measured.

The characteristic features of the apparatus are (1) that all moments and motions are taken around a system of three body axes which intersect at one point, (2) that the forcing motion is not affected by deflections in the planes of the two forced motions, (3) that the system is fairly rigid in the planes of the two forced motions, thus reducing the effect of unsymmetrical deflections under load and alleviating the requirement for a very small static margin in the plane of the non-rolling forced motion and, (4) that semiconductor gages and lock-in amplifiers are used for obtaining outputs representing the two forced motions, permitting the extraction of even very weak signals as long as they are synchronous with the forcing motion.

A set of two experiments is required to obtain, from the in-phase and quadrature components of the two forced motions, a complete set of 4 static cross-derivatives ($C_{m\beta}$, $C_{n\alpha}$, $C_{l\alpha}$ and $C_{l\beta}$) and 4 dynamic cross-derivatives ($C_{mr} - C_{m\beta} \dot{\cos\alpha}_0$, $C_{nq} + C_{n\alpha} \dot{}$, $C_{lq} + C_{l\alpha} \dot{}$ and $C_{lr} - C_{l\beta} \dot{\cos\alpha}_0$). The same two experiments also provide a complete set of direct, one-degree-of-freedom, derivatives, namely

the two static derivatives $C_{m\alpha}$ and $C_{n\beta}$, and the two damping derivatives $C_{mq} + C_{m\dot{\alpha}}$ and $C_{nr} - C_{m\dot{\beta}} \cos \alpha_0$. This latter information is obtained from the torque, amplitude and frequency characteristics of the forcing motion, using methods described in Reference 5. All derivatives are defined in the body system of axes and represent the aerodynamic moments due to small deflections and small rates of change of the deflections from an arbitrary set of a nominal angle of attack α_0 and a nominal angle of sideslip β_0 .

3. MECHANICAL ARRANGEMENT

3.1 Design Considerations

The basic part of the apparatus contains three cruciform flexures to provide degrees of freedom in pitch, yaw and roll (Figure 1). A one-piece construction is used to eliminate the effects of mechanical joints. The axes of the flexures are orthogonal, the origin being fixed with respect to the supporting sting. The model is attached to a flange on the front end of the flexure unit which in turn is secured rigidly to the sting.

An electromagnetic exciter drives the unit at an amplitude of up to 2° in pitch (or yaw). The required restoring moment in this plane is provided by a pair of auxiliary cantilever springs fastened to the moving part of the balance and attached to the sting through flexural pivots.

With the exception of the cruciform flexures the balance unit was manufactured using conventional machining methods. For reasons of inaccessibility and complexity the cruciform sections proper were made by electrical discharge machining (EDM). The material used was 17-4 PH stainless steel, heat-treated to Rockwell C-38 prior to the EDM operation. This material was

selected because of its well-known structural and fatigue characteristics.

The balance unit is designed to accept a model that under static conditions and in an upright position can be exposed to the following load limitations: normal force 80 lb, side force 80 lb, axial force 20 lb, pitching moment 4.7 lb.in, yawing moment 5.5 lb.in and rolling moment 5.4 lb.in. The above moment limits are compatible with a maximum angular deflection of 1.5° in pitch and 0.5° in yaw and in roll. Mechanical stops are incorporated in the model to prevent overstressing due to excessive angular deflections, which may occur in the presence of negative damping or very large dynamic cross-derivatives as well as during the starting or stopping of the wind tunnel.

The present balance unit requires a model cavity in the form of a truncated cone with diameters 3.06 in. and 1.55 in. and height 4.35 in. The actual flexure unit, however, is considerably smaller, and it is possible that with a different driving mechanism the required model cavity could be reduced to a cylindrical space, 1.9 in. in diameter and 4.3 in. long.

The balance unit, completely instrumented and mounted on the sting, is shown in Figure 2.

3.2 Driving Mechanism

The model is oscillated with constant amplitude at its mechanical resonant frequency in the plane of forcing motion. A feedback system (described in Reference 6) provides the necessary power for the electromechanical driving mechanism, which consists of two semi-circular permanent magnets anchored to the supporting sting and a rigid, high-current (up to 50 A), single-turn coil free

to move within the air gaps between the magnets. The coil is attached to the balance in a manner that permits it to impart to the model a forcing motion in one plane, but is not subject to the resulting forced motions in the other two planes, thereby eliminating problems of lateral displacement within the narrow air gaps. A torque of up to 0.4 lb.in can be generated, which has proven to be sufficient to drive the model at resonance in all test conditions.

4. INSTRUMENTATION

The signals corresponding to the angular deflections around all three axes are obtained from strain gage bridges mounted on the respective cruciforms. Semiconductor gages are employed in the planes of the two forced motions in order to improve the signal-to-noise ratio of the pertinent output signals which usually represent amplitudes of the order of a tenth of a degree only.

A special effort was made, with considerable success, to minimize the induced and common-mode noise by using balanced lines in conjunction with suitable shielding and grounding techniques. These precautions are particularly important in view of the large current at the critical frequency flowing through the driving coil, which is unavoidably located near the sensing elements. The signals are nonetheless contaminated by noise of aerodynamic origin to such an extent that conventional filtering methods are rendered ineffective for the extraction of the necessary information.

However, the small amplitude of the mechanical oscillation of the model permits to assume that, for a given model attitude, the system is linear around its equilibrium position, in which case

the forced motions are sinusoidal and of the same frequency as that of the forcing motion. The a priori knowledge of the nature of these motions allows the use of more sophisticated signal extraction methods to obtain the information necessary for the eventual determination of aerodynamic derivatives. Figure 3 shows a block diagram of the system used to acquire the pertinent data. The system is centered around a two-phase lock-in amplifier system capable of extracting signals coherent with the reference one that are deeply buried in noise. The signal corresponding to the displacement of the forcing motion is used as the reference by virtue of its high signal-to-noise ratio. The in-phase and quadrature components of the forced motions relative to the forcing motion can thus be obtained.

Although the signal-to-noise ratio of the output signal of a lock-in amplifier can be improved by increasing the time constant of its RC post-detection filter, the run duration in an intermittent wind tunnel imposes an upper limit on the usable integration time. To permit the use of a longer time constant, the signals representing all three angular deflections are stored on a magnetic tape loop, so that they can be played back during a longer period of time. Although this subterfuge does not improve the accuracy of the results (which is only a function of the total time during which the data are collected), it provides easily-observable average values for a particular wind-tunnel run, which - if necessary - can then in turn be averaged with those of other runs. This problem, of course, would not exist in continuous-flow wind tunnels.

The additional instrumentation for measurement of the direct derivatives consists of a monitor of the driving coil current, a frequency counter, two RMS/DC converters and a divider module, to obtain the ratio of the forcing torque to angular amplitude, in a manner described in Reference 5.

A photograph of the instrumentation system employed is shown in Figure 4.

5. EXPERIMENTAL PROCEDURES

5.1 Bench Calibrations

The torque capability of the driving mechanism as function of coil current is determined by loading the end of a light beam attached to the coil and pivoting on a ball bearing. The current required to null the deflection is measured. Repeating the experiments for different positions of the coil within the air gap proved that the magnetic field within the region of interest is completely uniform.

The sensitivities and stiffnesses of the balance are obtained by static calibration, which is accomplished by suitably loading a calibration fixture (Figure 5) attached to the front flange of the balance. Deflections are measured with a cathetometer. Maximum calibration loads correspond to deflections of 2°.

The natural frequencies in the three degrees of freedom are found by measuring the oscillation frequency of the model after releasing it from a deflected position in each of its planes of motion. For this calibration the model is mounted (at 0° roll and also at 90° roll) on the actual balance-and-sting combination. It

is convenient to attach the sting to the support that is used in the wind tunnel, this support in turn being clamped rigidly to a large surface table. The natural frequencies together with the corresponding direct stiffnesses are then used to determine the moments of inertia of the system about the 3 axes.

The accuracy of the complete system is assessed by applying a known external torque in the planes of forced motion at the forcing frequencies. This is accomplished by means of the loading arrangements shown in Figures 6 and 7, for which the model is mounted on the surface table on its actual balance-and-sting combination. The frequency response of the system in yaw and in roll is determined by means of a variable-speed motor-driven external oscillator. An eccentric coupling driving a pair of calibrated strain-gaged cantilevers provides a known moment in yaw to the model; a moment in roll is imposed with another pair of cantilevers combined with a change in orientation of the driving motor.

5.2 Calibrations in the Wind Tunnel

The direct mechanical damping of the balance is obtained after installation in the wind tunnel, and is determined from the logarithmic decrement as the model is allowed to damp freely from a deflected position of about 2° in each of its planes of motion. These measurements are made in near vacuum (≈ 10 mm Hg) and used for data reduction. Similar, more-easily made measurements are performed in air and are repeated from time to time in the course of the experiments in order to detect any changes in the values obtained in vacuum.

5.3 Wind Tunnel Experiments

Tunnel runs of about 13 sec. duration are taken, during which the balance provides an amplitude-stabilized motion in the plane of the forcing motion (pitch or yaw). Outputs from the pitch, yaw and roll bridges are recorded on a closed loop of magnetic tape of such a length that the starting and stopping shock effects are eliminated. At the same time the ratio of the driving torque to the amplitude ($\sim 1.2^\circ$) as well as the driving phase angle are recorded on two strip-chart potentiometer recorders. Corresponding tare readings before each run are taken at a pressure of about 30 mm Hg and recorded on a separate loop of tape. The model is tested in the pitch attitude and, by rotating it 90° on the balance, also in the yaw attitude.

For the determination of cross-derivatives, the in-phase and quadrature voltage outputs of the roll and yaw (or pitch) bridges, referenced to the pitch (or yaw) bridge output are obtained by playing back the tape loops into the lock-in amplifier. Because of the short tunnel runs two or three runs are usually required at each model attitude (given as a combination of angle of attack and angle of yaw) for averaging purposes.

The direct derivatives are obtained from the forcing motion using the strip-chart recorder readings together with the frequency of oscillation as measured with a commercial counter.

6. DATA REDUCTION

6.1 General

Each wind tunnel test provides sufficient data to determine the direct derivatives associated with the forcing motion in pitch (or yaw) and part of the information necessary for the determination

of the pertinent cross-derivatives. The remainder of such information is obtained from another test where the model is at the same aerodynamic attitude but oscillating in yaw (or pitch). A pair of such tests shall be denoted "complementary tests" in the following discussion. A flow diagram describing the data reduction is shown in Figure 8, although it should be noted that the data generated from a complementary pair of tests leads to the use of two such charts [e.g. Test A (procedure I) coupled with test B (procedure II) and Test A (procedure II) coupled with test B (procedure I)].

Procedure I yields the direct derivatives and the aerodynamic moments required in the determination of the cross-derivatives. Procedure II combines the data originating from the forced planes (induced or secondary motions) with the moments obtained from procedure I to determine the cross-derivatives.

Vector notation is used to represent sinusoidal time variations of deflections, moments, etc. All phases are referred to the deflection in the forcing plane.

6.2 Direct derivatives

The direct aerodynamic static and dynamic derivatives are obtained by the well-known single-degree-of-freedom constant-amplitude oscillation technique. The data obtained from the test are (for oscillation-in-pitch):

- Oscillation amplitude, θ , and frequency, ω
- Amplitude of forcing torque, M_y
- Phase angle, χ , between forcing torque and deflection in the forcing plane.

The aerodynamic moments in the plane are given by (Reference 7)

$$M_{\dot{\theta}} = - \left(\frac{M_Y \sin \chi}{\omega \theta} - \frac{M_{Y,o} \sin \chi_o}{\omega_o \theta_o} \right) \quad (1)$$

$$M_{\theta} = - I_Y (\omega^2 - \omega_o^2) - \left(\frac{M_Y}{\theta} \cos \chi - \frac{M_{Y,o}}{\theta_o} \cos \chi_o \right) \quad (2)$$

where subscript "o" denotes vacuum tare conditions. This leads to the following direct derivatives:

$$C_{m\alpha} = \frac{1}{\bar{q} A_b \ell} M_{\dot{\theta}}$$

$$C_{mq} + C_{m\dot{\alpha}} = \frac{2V}{\bar{q} A_b \ell^2} M_{\theta}$$

Similar expressions are used for the direct derivatives in yaw, $C_{n\beta}$ and $(C_{nr} - C_{n\beta} \cos \alpha_o)$.

6.3 Cross-derivatives

The model is oscillated in yaw (or pitch) at an attitude $\alpha = \alpha_o$, $\beta = \beta_o$ (therefore in the complementary test the model oscillates in pitch (or yaw) at $\alpha = \alpha_o$, $\beta = \beta_o$).

The approach followed for the processing of the data is based on the following assumptions:

(i) The aerodynamic and mechanical interactions between the forced motions can be neglected by virtue of the very small deflections in those planes (relative to that of the forcing motion) resulting from the high associated stiffnesses. Likewise the primary motion is not affected by the secondary ones.

(ii) The vacuum tare and wind-on amplitudes of the forcing oscillation are approximately equal due to the high stiffness of the driving servo system. In a few cases where the wind-on amplitudes were slightly lower, the output data were multiplied by the amplitude ratio.

The experimental data required for procedure II are the sinusoidal components coherent with the forcing oscillation, of the vacuum tare and wind-on deflections in the planes of forced motion in pitch (or yaw) and roll.

By subtracting the tare vectors from the corresponding wind-on ones, the deflections due to aerodynamic effects are obtained (aerodynamic vectors).

These deflections are assumed to represent the response of second order systems to an excitation by sinusoidal forcing moments synchronous with the primary motion. It is therefore necessary to convert the measured deflections into such forcing moments before the aerodynamic moments associated with the desired cross-derivatives can be determined.

The equation of motion for a second order system can be written

$$m\ddot{X} + c\dot{X} + kX = P \sin\omega t \quad (3)$$

which rewritten for a pitching moment, is

$$\ddot{\theta} + \left[\frac{\gamma_{\theta} - M_{\dot{\theta}}}{I_Y} \right] \dot{\theta} + \left[\frac{k_{\theta} - M_{\theta}}{I_Y} \right] \theta = \frac{M}{I_Y} \sin\omega t \quad (4)$$

or
$$\ddot{\theta} + \mu_{\theta} \dot{\theta} + \omega_{\theta}^2 = (M/I_Y) \sin\omega t$$

Therefore to obtain the damping coefficient μ_{θ} , the aerodynamic damping derivative $M_{\dot{\theta}}$ is required, which is obtained from the complementary test. γ_{θ} and I_Y are determined separately. Likewise M_{θ} is obtained from the complementary test and combined with k_{θ} and I_Y to generate the proper wind-on resonant frequency (ω_{θ}). It should be noted that the resonant frequency, mechanical damping and moment of inertia in pitch depend on the position of the model relative to the balance unit and are therefore subscripted in Figure 8 to denote the pertinent test conditions. A similar

procedure is followed to obtain μ_ψ and ω_ψ in the yawing plane.

In the case of the rolling plane, a theoretical value of L_p (obtained by procedures described in Reference 8) must be used since the damping-in-roll cannot be determined experimentally with the present apparatus. Furthermore, the undamped resonant frequency in roll, $(\omega_n)_\phi$, is used because the aerodynamic restoring moment in roll for the relatively small angles of attack and sideslip of the present tests can be assumed negligible, particularly in view of the fact that the rolling resonant frequency ω_ϕ is considerably higher than the forcing frequency ω and, consequently, small changes in the rolling frequency have no effect on the final result.

The modulus of the forced moment in pitch (M_y in Eqn. 4), when the model is oscillated in yaw with the forcing frequency ω , is given for an underdamped system, such as the one under consideration, by (Reference 9)

$$M_y = Ak_\theta \sqrt{\left[1 - \frac{\omega^2}{\omega_\theta^2}\right]^2 + \frac{\mu_\theta^2 \omega^2}{\omega_\theta^4}} \quad (5)$$

where A is the modulus of the aerodynamic pitch vector, and ω_θ , as before, is the resonant damped frequency in pitch with the model mounted in the proper position (i.e. for oscillation-in-yaw).

The phase angle between M_y and A is obtained as

$$\epsilon = \text{arc tan} \frac{\mu_\theta \omega}{\omega_\theta^2 - \omega^2} \quad (6)$$

All the terms on the right-hand side of the equations are known and therefore the aerodynamic moment vectors can be determined. The corresponding static and dynamic cross-derivatives are then readily obtained from the in-phase and quadrature components (real and imaginary parts) of these vectors, by reducing them to standard non-dimensional forms (Figure 8).

7. WIND TUNNEL AND MODEL

The experiments were performed in the NAE 30 in. x 16 in. intermittent suction wind tunnel at a Mach number of 2.0. Tunnel stagnation pressure was approximately atmospheric (14.0 psia) and the stagnation temperature was close to ambient (averaging about 80°F). The intake air was dried to a specific humidity of about 0.001. The Reynolds number per foot was 3.6×10^6 . Transverse variation of Mach number at the model location in the empty tunnel was less than ± 0.01 and the longitudinal variation was ± 0.02 .

The model was made of aluminium alloy, the body and wing being machined in one piece. The fin was brazed on the body in a final operation. The rear half of the body was hollowed out to a constant wall thickness of 0.055 in. to provide room for the driving mechanism. Mass balancing was achieved by drilling out the solid portion of the body forward of the attachment point.

Figure 9 gives the geometric characteristics of the model, while Figure 10 shows the model installed in the wind tunnel.

8. EXPERIMENTAL PROGRAM AND RESULTS

8.1 Program

The experiments consisted of oscillation-in-pitch and oscillation-in-yaw at the following combinations of the mean angle

of attack α_0 and the mean angle of sideslip β_0 :

$\beta_0 \backslash \alpha_0$	0	5°	10°	15°
0	X	X	X	X
5°	X	X	X	X
10°	X	X	X	X
15°	X	X	X	

Each cross denotes two separate wind tunnel experiments, to provide forcing motion partly in pitch and partly in yaw. For α_0 and β_0 not exceeding 10°, the oscillation-in-yaw was arranged by turning the sting and its support by an angle α_0 sidewise and by an angle β_0 in a vertical plane, with the wings and the plane of oscillation oriented vertically. For $\alpha_0 = 15^\circ$ the oscillation in yaw was arranged by rotating the sting 90° and turning it, together with its support, by an angle β_0 sidewise and by an angle α_0 in a vertical plane, with the wings and the plane of oscillation tilted 15° to the horizontal. Similarly, for $\beta_0 = 15^\circ$ the oscillation-in-yaw was performed in a vertical plane and the oscillation-in-pitch in a lateral plane. In all other cases the oscillation (in pitch) was performed in a vertical plane in an attitude normal for wind tunnel tests. Since the sting and its

support could not easily be turned sidewise by more than 10° , no experiments were undertaken for the case $\alpha_0 = 15^\circ$, $\beta_0 = 15^\circ$.

In most cases the amplitude of the forcing motion was 1.2° and the frequency 35 - 40 Hz. Apart from some studies of repeatability of the results, most experiments were repeated twice or three times, to compensate for the very short duration of the wind tunnel runs.

8.2 Results

The results of all the individual experiments carried out are presented in Table 1. Both the direct derivatives and the cross-derivatives are shown for pitching experiments as well as for yawing experiments. Both the static and the dynamic data are included. When calculating the cross-derivatives for an individual experiment, the average value of the direct derivatives from the complementary experiment was used. It was observed that for the frequencies and damping factors involved in this investigation, the effect of the direct derivatives on the resulting cross-derivatives of the complementary experiments was not negligible, although in most cases it was small.

The number of individual experiments belonging to the same set of nominal test conditions (α_0, β_0) varies greatly, depending on the scatter of the results; in some cases a larger than normal number of experiments was employed simply to investigate in more detail the repeatability of results. In no case is the number of individual experiments less than two. These repeated experiments were part of the acceptance procedure for the new apparatus and were made necessary due to the very short run time of the intermittent wind tunnel used. It is envisaged that in a continuous-flow facility no such repeats would be necessary.

The final results of the experimental program are presented in Table 2. These results were calculated by averaging the aerodynamic vectors determined during the individual experiments and by applying the data reduction procedure to the resulting average values. The final results are therefore not necessarily equal to the average of the results of individual experiments, previously given in Table 1, although in most cases they are quite close.

Both the direct derivatives and the cross-derivatives are plotted in Figures 11 and 12 as functions of α_0 with β_0 as parameter and in Figures 13 and 14 as functions of β_0 with α_0 as parameter. Figures 11 and 13 show the dynamic derivatives and Figures 12 and 14 show the static ones.

8.3 Additional Experiments on Cones

It was initially planned to include in the program some experiments on a 10° cone with a nose asymmetry. Preliminary tests, not reported here, were performed both on a pointed cone and on a cone with two different nose asymmetries. It was found that even at angles of attack of the order of 35° (but at zero sideslip) the cross-derivatives remained very small, and therefore of no particular interest. It was therefore decided to extend instead the initial program on the cone-wing-fin configuration to also include some experiments at $\alpha_0 = 15^\circ$ and at $\beta_0 = 15^\circ$, where larger variations in some of the derivatives could be expected.

9. SUMMARY AND CONCLUSIONS

A new wind tunnel apparatus has been developed and constructed for the determination of moment cross-derivatives due to pitching and yawing on aircraft models at moderate angles of attack and sideslip. The apparatus can also be used to determine the direct moment derivatives in pitch and yaw. Experimental results were obtained at Mach 2 on a cone-wing-fin configuration at angles of attack and sideslip up to 15° in a 30 inch intermittent wind tunnel. Even if in most cases the dynamic cross-derivatives measured were very small, quite satisfactory repeatability of results was in general obtained. On that basis it appears that dynamic cross-derivatives as small as 0.002 in the case of those due to pitching and as small as 0.001 in the case of those due to yawing can be determined with the present experimental set-up. These figures may, however, depend strongly on the various experimental quantities, such as frequency ratios, signal-to-noise ratios and the duration of the experiments, all of which may vary significantly with the model, balance stiffness, sting support and the wind tunnel used.

Although in most cases investigated the dynamic derivatives were very small, measurable effects were sometimes observed, at all angles of attack included in this investigation (i.e. up to 15°), when the angle of sideslip was 10° or 15° . For dynamic cross-derivatives $(C_{\ell q} + C_{\ell \dot{\alpha}})$, $(C_{m r} - C_{m \beta} \cos \alpha_0)$ and $(C_{n q} + C_{n \dot{\alpha}})$ [which represent the coupling between the lateral and the longitudinal degrees of motion] these effects were of the order of up to 5 percent of the direct damping derivative in the pertinent equation of motion and can probably be expected to be even larger for

higher values of angles of attack and sideslip and for configurations more prone to asymmetric vortex shedding (such as a winged configuration with a long forebody). If so, it may be desirable to include such derivatives in the flight mechanics analysis of aircraft flying at moderate angles of attack and sideslip, such as may be encountered during certain high performance maneuvers, when using direct lift or side-force control, or during certain phases of spin motion. To the best knowledge of the present authors, the three cross-derivatives in question have never been determined before.

10. ACKNOWLEDGEMENT

The authors wish to acknowledge the contribution to this project of several members of the Unsteady Aerodynamics Laboratory staff and especially of Mr. D.M. Finn (theoretical calculations and data reduction), Mr. L.T. Conlin (mechanical design), Messrs. E. Peter and B.E. Moulton (construction of parts and models, calibration and wind tunnel work), Mr. R.Foster, (instrumentation and strain gaging) and last but not least of Mrs. M. McCooeye (data reduction and diagrams) and Mrs. S. Adamson (typing). The project was of an exploratory nature, and therefore often caused unforeseen problems, and it was only due to the interest and enthusiasm of all the members of the team that it was brought to a satisfactory completion.

11. REFERENCES

1. Tobak, M.
Schiff, L.B. A nonlinear aerodynamic moment formulation and its implication for dynamic stability testing; AIAA Paper 71-275, March 1971.
2. Schiff, L.B.
Tobak, M. Results from a new wind-tunnel apparatus for studying coning and spinning motions of bodies of revolution; AIAA Journal, Vol. 8, No. 11, Nov. 1970, pp. 1953-1957.
3. Orlik-Rückemann, K.J. Survey of needs and capabilities for wind tunnel testing of dynamic stability of aircraft at high angles of attack; NASA CR 114583, March 1973.
4. Orlik-Rückemann, K.J. Dynamic stability testing of aircraft -- needs versus capabilities. Proceedings of the 5th International Congress on Instrumentation in Aerospace Simulation Facilities, Pasadena, California, September 1973.
5. Orlik-Rückemann, K.J.
LaBerge, J.G.
Hanff, E.S. Supersonic dynamic stability experiments on the space shuttle; AIAA Paper 72-135, January 1972.
6. Orlik-Rückemann, K.J.
Adams, P.A.
LaBerge, J.G. On dynamic stability testing of unconventional configurations; AIAA Paper 71-276, March 1971.

7. Orlik-Rückemann, K.J. Wind tunnel measurements of dynamic derivatives, Lecture Notes, UCLA 1963.
8. Ellison, D.E. USAF Stability and Control Datcom
Hoak, D.E. WADD TR-60-261
(continuously revised)
9. Timoshenko, S. Vibration problems in engineering
D. Van Nostrand Co., New York 1937.

Results of individual runs (mean values of direct derivatives from complementary tests used in calculations)

α_0 deg	β_0 deg	OSCILLATION-IN-PITCH						OSCILLATION-IN-YAW					
		$C_{lq} + C_{l\dot{\alpha}}$	$C_{nq} + C_{n\dot{\alpha}}$	$C_{l\alpha}$	$C_{n\alpha}$	$C_{mq} + C_{m\dot{\alpha}}$	$C_{m\alpha}$	$C_{lr} - cC_{l\beta}$	$C_{mr} - cC_{m\beta}$	$C_{l\beta}$	$C_{m\beta}$	$C_{nr} - cC_{n\beta}$	$C_{n\beta}$
0	0	-.0011	.00006	-.0137	-.006	-1.33	.027	.0016	.0024	.203	-.007	-.253	.044
		.0003	-.00045	-.0141	.001	-1.28	.026	.0050	.0028	.211	-.010	-.255	.042
0	5	.0011	.0062	-.196	-.036	-1.01	.036	.0037	.0013	.126	-.0059	-.384	.040
		.0014	.0056	-.196	-.036	-1.01	.032	.0038	.0021	.125	-.0029	-.366	.047
0	10	.0030	.0049	-.193	-.037	-1.01	.031	.0053	.0009	.125	-.0092	-.382	.035
		.0029	.0047	-.192	-.041	-1.04	.027	.0050	.0029	.121	-.0060	-.392	.037
0	15	.0028	.0047	-.174	-.055	-.95	.034	.0045	.0019	.121	-.0060	-.380	.036
		.0019	.0043	-.176	-.050	-.99	.021						
5	0	.0010	.0054	-.172	-.051	-1.01	.026						
		.0062	.0146	-.354	-.093	-1.12	.038	.0024	.0033	.117	-.012	-.299	.048
5	5	.0062	.0143	-.354	-.085	-1.19	.031	.0020	.0029	.113	-.016	-.294	.049
		.0004						.0004	.0033	.110	-.013	-.290	.050
5	10	.043	.0020	-.90	.017	-1.32	-.209	.0037	.0057	.168	.059	-.189	.161
		.026	.0024	-.90	.019	-1.31	-.190	.0073	.0051	.172	.041	-.197	.175
5	15	.028	.0018	-.89	.018	-1.32	-.198	.0059	.0064	.165	.042	-.156	.161
		-.00006	-.0009	-.013	.016	-.93	.064	.0056	-.0001	.239	.016	-.375	.038
5	5	-.00016	0	-.014	.018	-.98	.069	.0051	-.0001	.241	.013	-.367	.041
		-.00010	-.0007	-.010	.017	-.95	.063	.0049	-.0004	.244	.015	-.366	.034
5	10	-.00012	-.0033	-.021	.027	-.95	.067						
		-.00011	-.0035	-.019	.027	-.89	.070						
5	15	.00019	-.0029	-.019	.026	-.89	.077						
		.00032	-.0017	-.017	.017	-.93	.068						
5	5	.0040	-.0060	-.193	.029	-1.13	.070	.0022	-.0006	.283	-.010	-.374	.040
		.0032	-.0062	-.196	.025	-1.12	.071	.0031	.0020	.303	-.008	-.346	.036
5	10	.0033	-.0041	-.198	.027	-1.11	.050	.0040	.0021	.302	-.009	-.366	.034
		.0042	-.0055	-.199	.028	-1.12	.053	.0034	.0005	.300	-.010	-.350	.038
5	15	.0041	-.0055	-.195	.032	-1.14	.064	.0048	.0014	.298	-.004	-.347	.035
		.0032	-.0067	-.193	.032	-1.12	.055	.0053	.0015	.305	-.006	-.351	.034
5	5	.0040						.0040	.0003	.300	-.001	-.372	.037
		.0041						.0041	.0015	.307	.003	-.369	.036
5	10	.0053						.0053	.0003	.302	.010	-.357	.040
		.0028						.0028	.0018	.296	.002	-.363	.035
5	15	-.0040	-.015	.233	.143	-.83	.046	-.0029	.0029	.33	-.015	-.351	.046
		-.0031	-.015	.233	.142	-.77	.039	-.0027	.0033	.36	-.016	-.322	.045
5	5	-.0039	-.009	.222	.114	-.83	.053						
		-.0023	-.013	.230	.110	-.83	.055						

$c = \cos \alpha_0$

TABLE 1 (concluded)
 Results of individual runs (mean values of direct derivatives from complementary tests used in calculations)

α_0 deg	β_0 deg	OSCILLATION-IN-PITCH						OSCILLATION-IN-YAW					
		$C_{lq} + C_{l\dot{\alpha}}$	$C_{nq} + C_{n\dot{\alpha}}$	$C_{l\alpha}$	$C_{n\alpha}$	$C_{mq} + C_{m\dot{\alpha}}$	$C_{m\alpha}$	$C_{lr} - cC_{l\beta}$	$C_{mr} - cC_{m\beta}$	$C_{l\beta}$	$C_{m\beta}$	$C_{nr} - cC_{n\beta}$	$C_{n\beta}$
5	15	-.0032	-.0068	-.323	-.203	-1.70	-.21	.0037	.0140	.42	.213	-.239	.143
		-.0013	-.0090	-.317	-.201	-1.64	-.18	.0036	.0139	.42	.211	-.217	.161
10	0	.0002	.0009	-.003	-.025	-.76	.077	.0030	-.0038	.37	.011	-.386	.047
		-.0007	.0004	-.006	-.023	-.70	.080	.0025	-.0027	.32	.006	-.380	.043
		-.0004	.0010	-.003	-.025	-.68	.074	.0012	-.0025	.33	-.001	-.396	.040
								.0021	-.0020	.36	-.010	-.423	.059
							.0034	-.0021	.29	.014	-.378	.049	
10	5	.0009	-.0037	-.034	-.023	-.55	.056	.0046	.0039	.375	-.018	-.342	.038
		.0004	-.0035	-.035	-.020	-.58	.053	.0060	.0031	.371	-.022	-.327	.046
		.0017	-.0052	-.033	-.025	-.58	.050	.0068	.0022	.375	-.020	-.315	.044
								.0068	.0024	.375	-.021	-.304	.046
10	10	.0038	.0033	-.323	-.208	-.60	.026	.0076	.0265	.40	.009	-.320	.064
		.0018	.0021	-.328	-.205	-.60	.022	.0072	.0273	.38	.010	-.334	.074
10	15							-.0021	.0037	.39	.218	-.189	.227
								.0024	.0038	.40	.220	-.179	.217
								.0026	.0031	.42	.223	-.162	.189
15	0	.0005	-.0030	-.0023	.0044	-.75	.044	.0024	.0004	.45	-.007	-.341	.009
		.0001	-.0022	-.0014	.0044	-.76	.046	.0006	.0003	.46	-.006	-.419	-.013
15	5	.0002	0	-.009	-.035	-.87	-.079	-.0125	.0026	.48	-.323	-.459	
		0	-.0007	-.009	-.042	-.81	-.083	-.0099	.0012	.45	-.336	-.440	
15	10	-.0057	.014	-.361	-.203	-.89	-.151					-.542	
		-.0025	.002	-.369	-.206	-.68	-.110					-.554	
												-.650	

$c = \cos\alpha_0$

TABLE 2

Final results (based on averaged aerodynamic vectors for each test case)

α_0 (deg)	β_0 (deg)	OSCILLATION-IN-PITCH						OSCILLATION-IN-YAW					
		$C_{\dot{\alpha}} + C_{\dot{\alpha}} \dot{\alpha}$	$C_{n\dot{\alpha}} + C_{n\dot{\alpha}} \dot{\alpha}$	$C_{\dot{\alpha}} \alpha$	$C_{n\alpha}$	$C_{m\dot{\alpha}} + C_{m\dot{\alpha}} \dot{\alpha}$	$C_{m\alpha}$	$C_{\dot{\alpha}} r - c C_{\dot{\alpha}} \dot{\beta}$	$C_{m\dot{\alpha}} - c C_{m\dot{\alpha}} \dot{\beta}$	$C_{\dot{\alpha}} \beta$	$C_{m\beta}$	$C_{nr} - c C_{nr} \dot{\beta}$	$C_{n\beta}$
0	0	< .001	< .0005	-.014	-.002	-1.30	.026	.003	.0025	.206	-.008	-.256	.042
0	5	.002	.0050	-.184	-.045	-1.00	.029	.004	.0018	.124	-.006	-.381	.039
0	10	.006	.0144	-.354	-.089	-1.15	.034	.002	.0032	.114	-.014	-.294	.049
0	15	.032	.0021	-.90	.018	-1.32	.199	.006	.0058	.169	.047	-.181	.165
5	0	< .0003	-.002	-.016	.021	-.92	.067	.005	-.0002	.242	.015	-.370	.038
5	5	.0038	-.006	-.196	.029	-1.12	.061	.004	.0010	.300	-.003	-.355	.036
5	10	-.0033	-.013	.229	.127	-.82	.048	-.003	.0031	.34	-.016	-.336	.046
5	15	-.0022	-.008	-.320	-.202	-1.67	.192	.004	.0140	.42	.21	-.228	.152
10	0	< .001	< .001	-.005	-.024	-.71	.077	.002	-.003	.33	.006	-.392	.047
10	5	.001	-.004	-.034	-.023	-.57	.053	.006	.0031	.374	-.020	-.322	.043
10	10	.003	.003	-.326	-.206	-.60	.024	.007	.027	.39	.009	-.327	.069
10	15							.001	.0035	.404	.221	-.178	.211
15	0	.0003	-.0026	-.002	.004	-.75	.045	.001	.0003	.46	-.007	-.380	-.002
15	5	< .0003	< .0003	-.009	-.039	-.84	-.081	-.012	.0019	.47	-.33	-.449	
15	10	-.004	.008	-.361	-.205	-.78	-.130					-.58	

$$c = \cos \alpha_0$$

Direct
DerivativesDirect
Derivatives

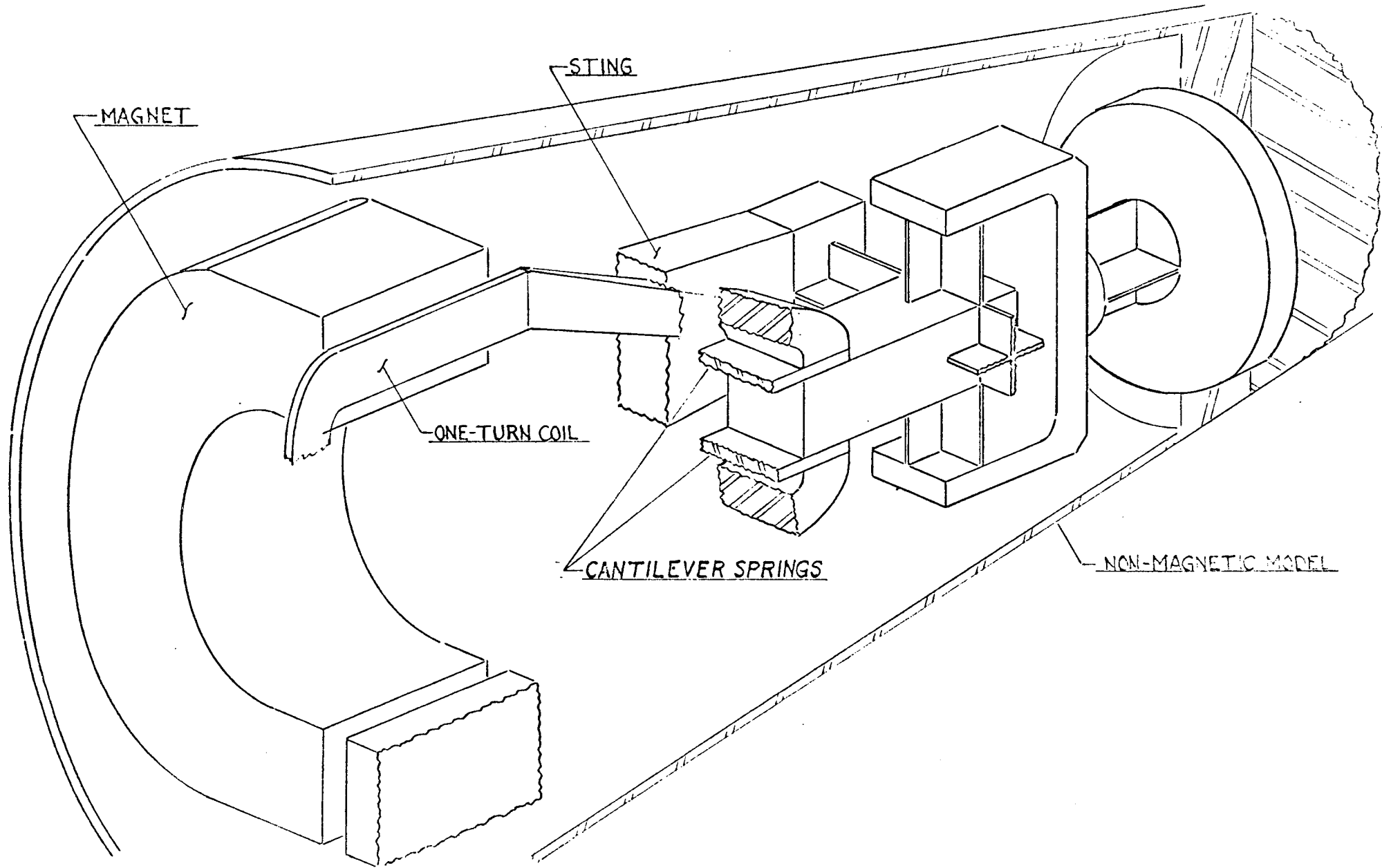


FIG. 1 - Schematic of Apparatus for Measurement of Cross-Derivatives

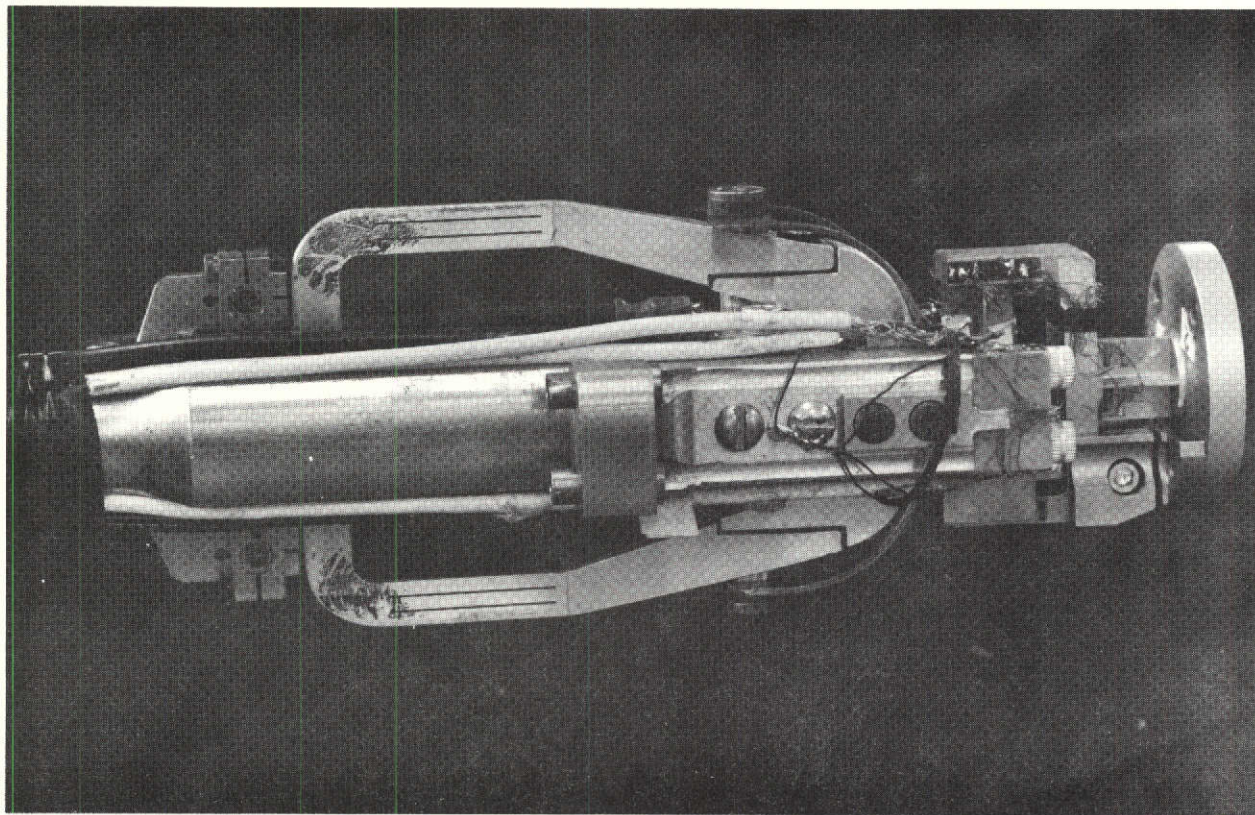


FIG. 2 Balance before attachment of model and permanent magnets.

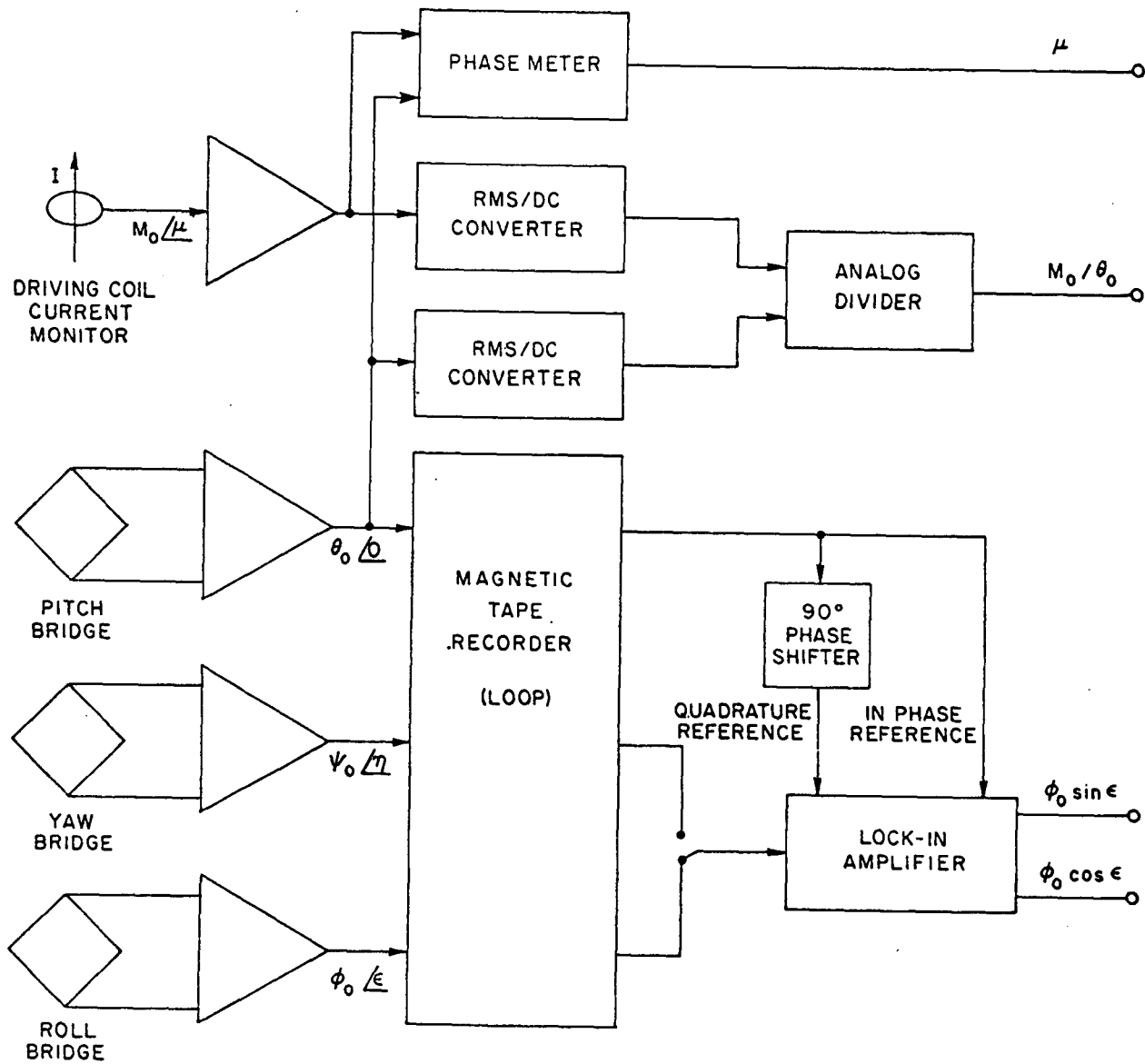


FIG. 3 Instrumentation System

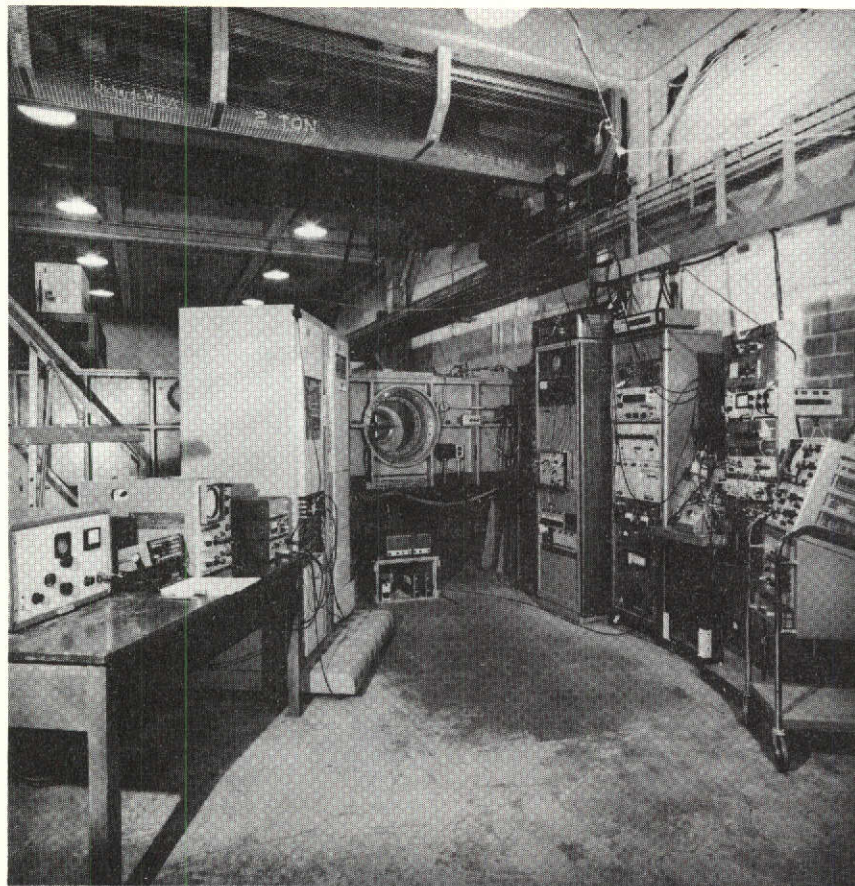


FIG. 4 General view of the experimental area showing the model in wind tunnel and the instrumentation system.

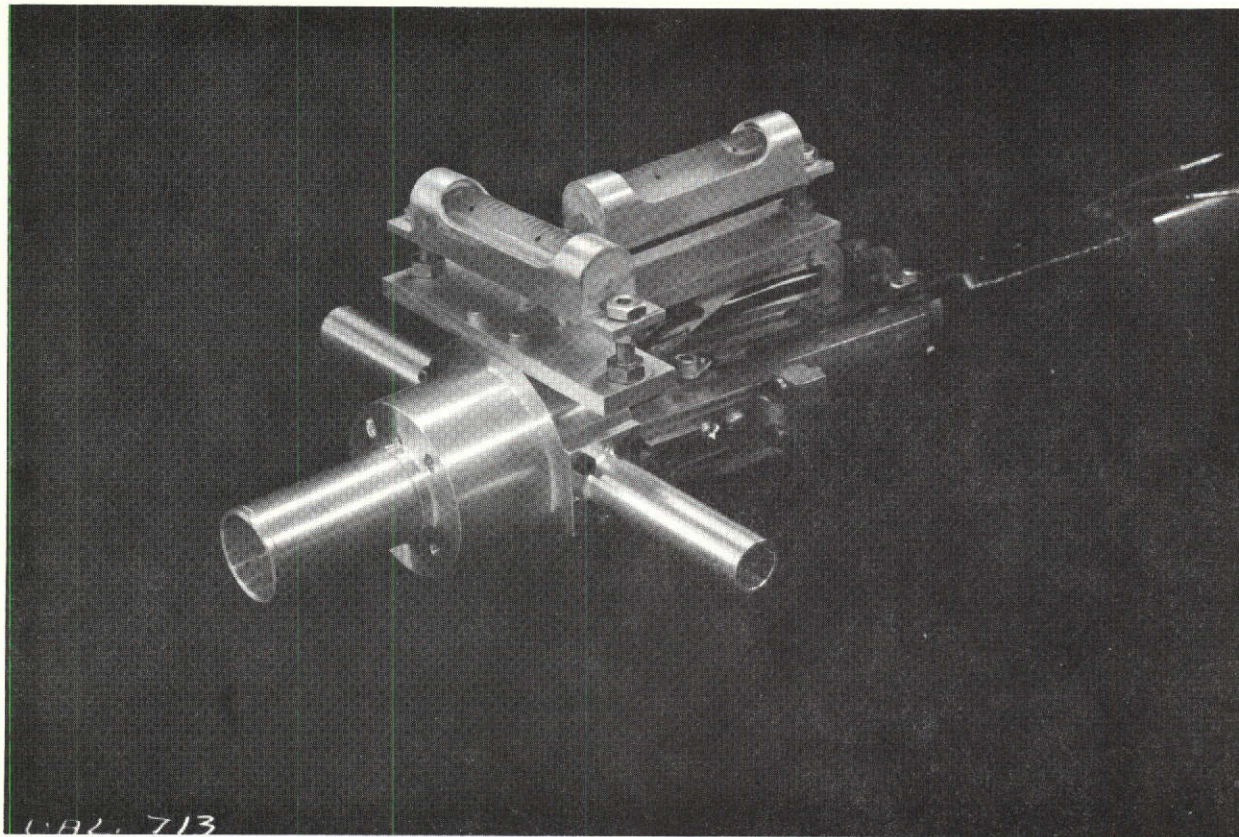


FIG. 5 Loading fixture for static calibration installed on balance.

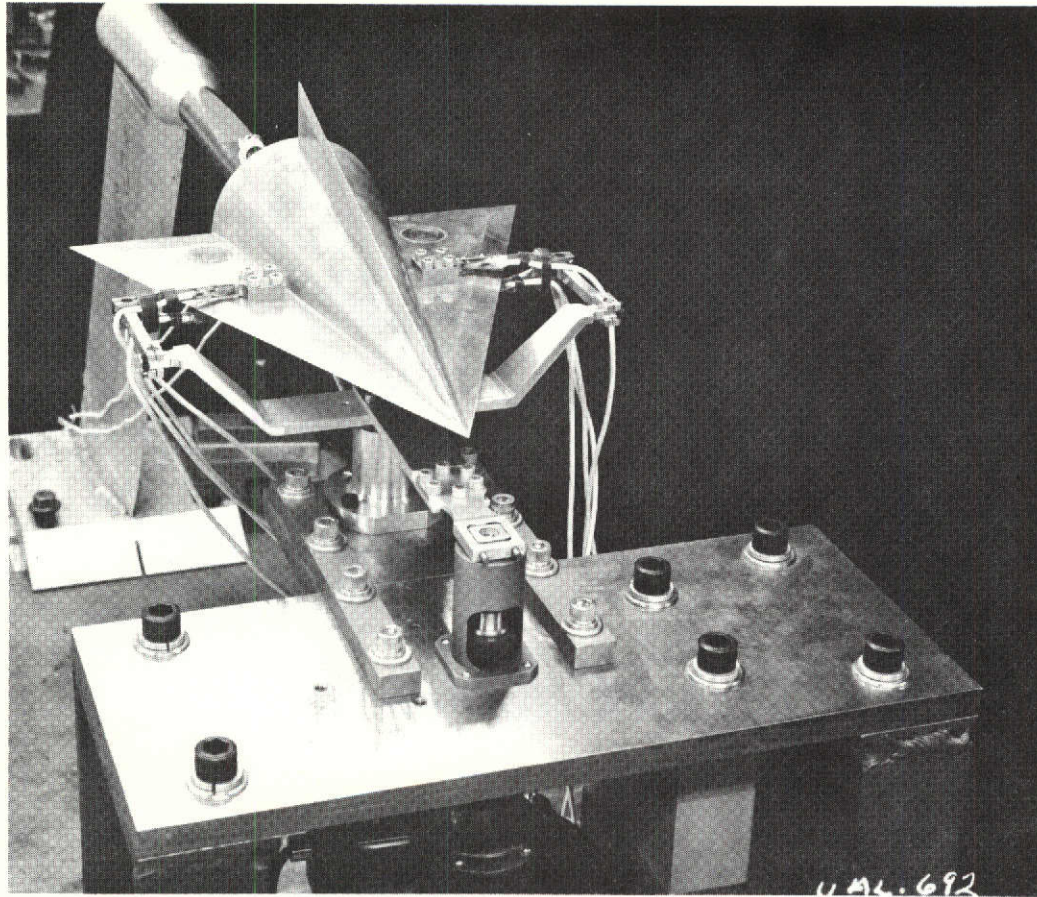


FIG. 6 Arrangement for dynamic calibration in yaw.

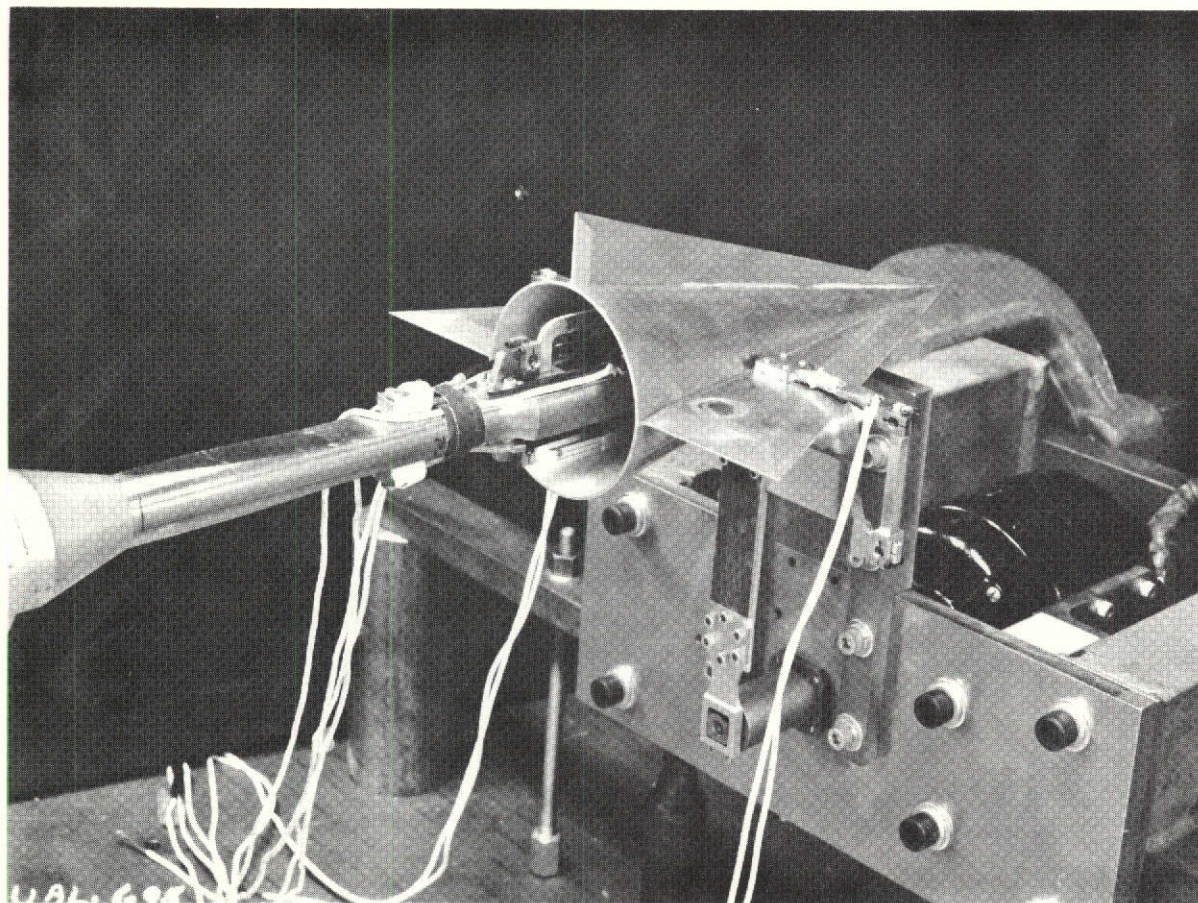


FIG. 7 Arrangement for dynamic calibration in roll.

COMPLEMENTARY TESTS

I. MODEL OSCILLATES IN PITCH

FORCED PLANES : YAW & ROLL

$$\alpha = \alpha_0 \quad \beta = \beta_0$$

VACUUM & WIND ON

II. MODEL OSCILLATES IN YAW

FORCED PLANES : PITCH & ROLL

$$\alpha = \alpha_0 \quad \beta = \beta_0$$

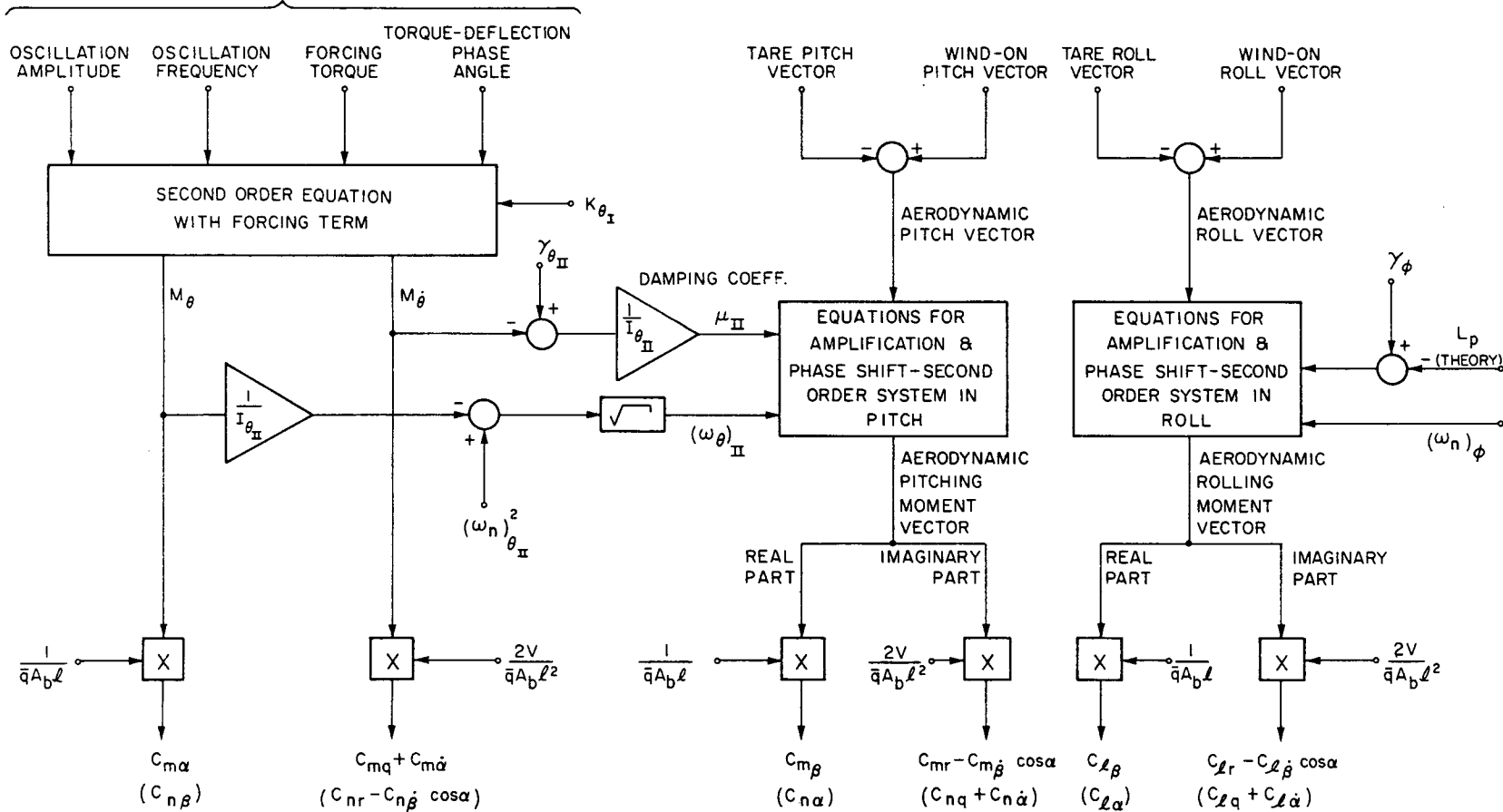


FIG.8 : FLOW PATTERN FOR DATA REDUCTION. DERIVATIVES IN BRACKETS SIMILARLY OBTAINED BY APPLYING PATTERN I TO OSCILLATION IN YAW AND PATTERN II TO OSCILLATION IN PITCH

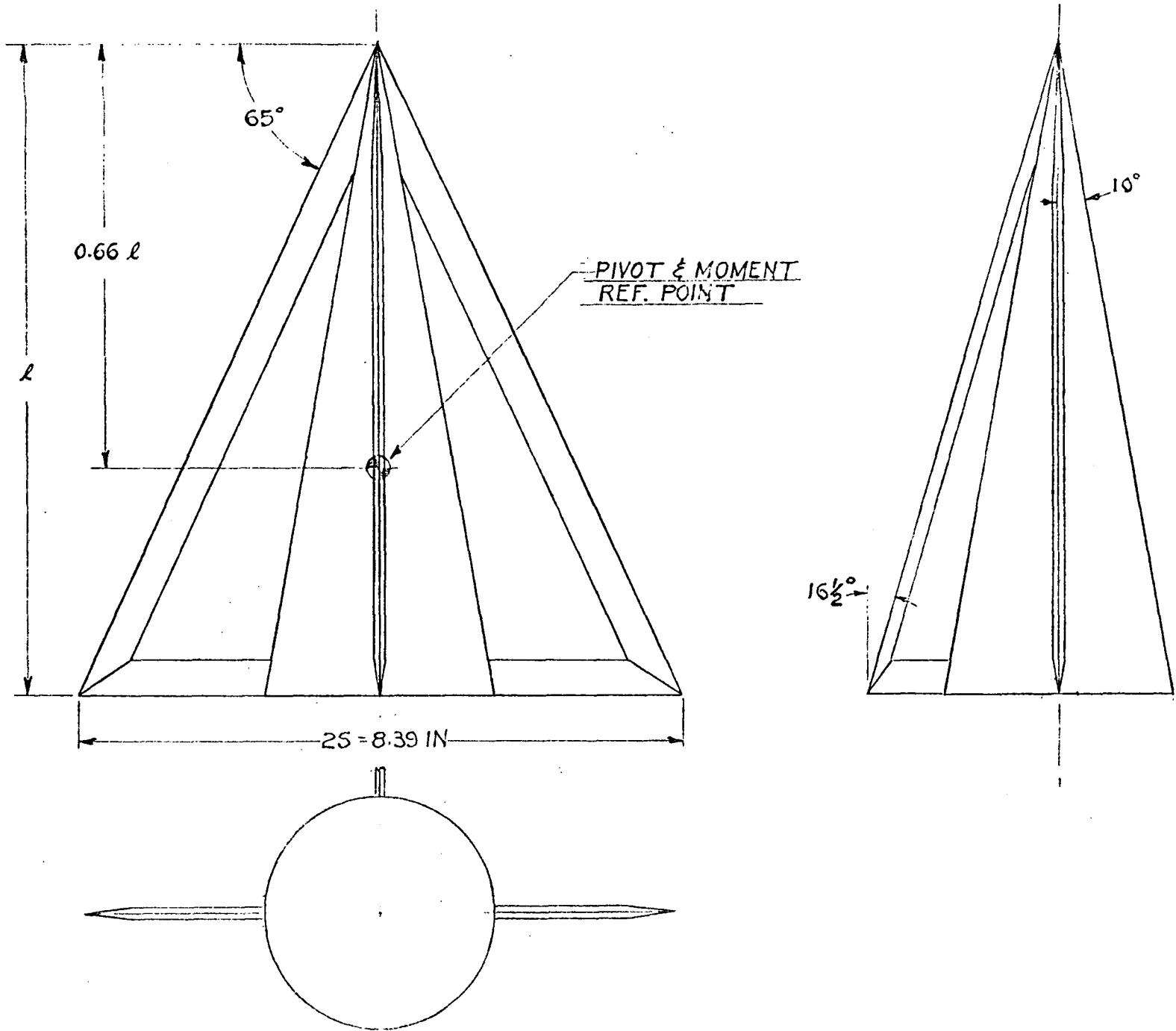


FIG. 9 Outside dimensions of the cone-wing-fin model.

β
 0° ○
 5° □
 10° △
 15° ◇

$\bar{x}_0 = 0.66, M = 2.0$

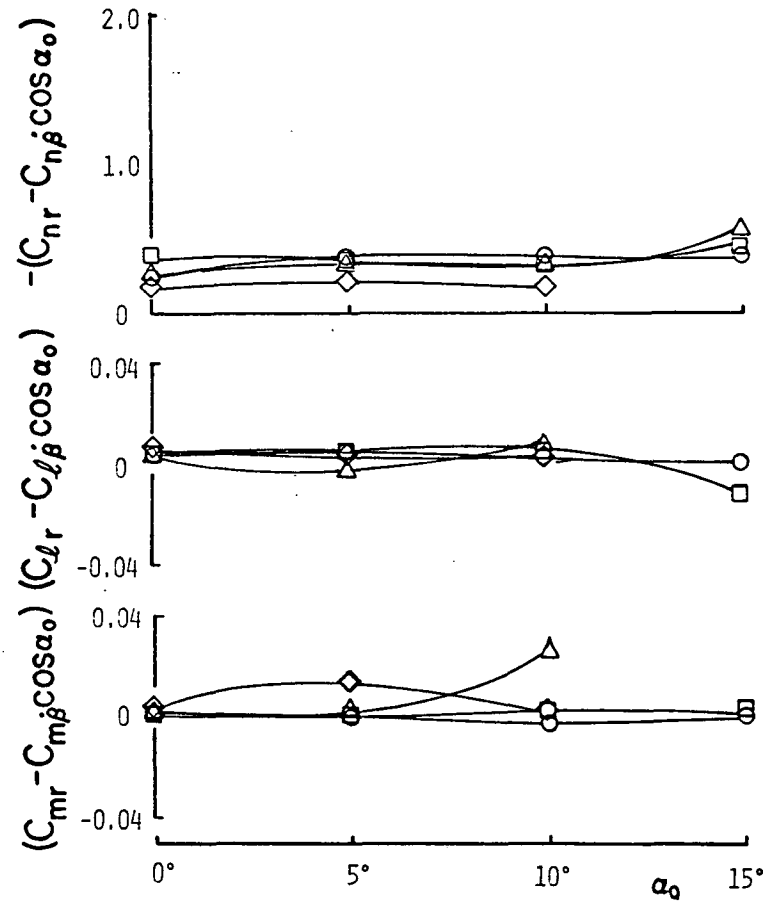
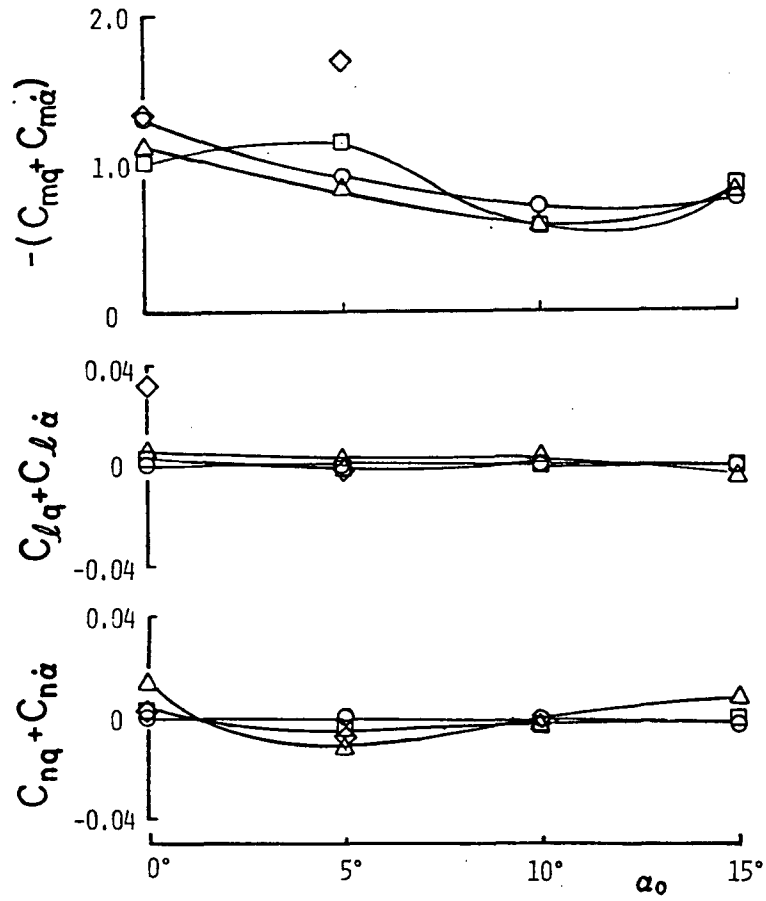


FIG. 11 DYNAMIC DERIVATIVES AS FUNCTION OF α_0

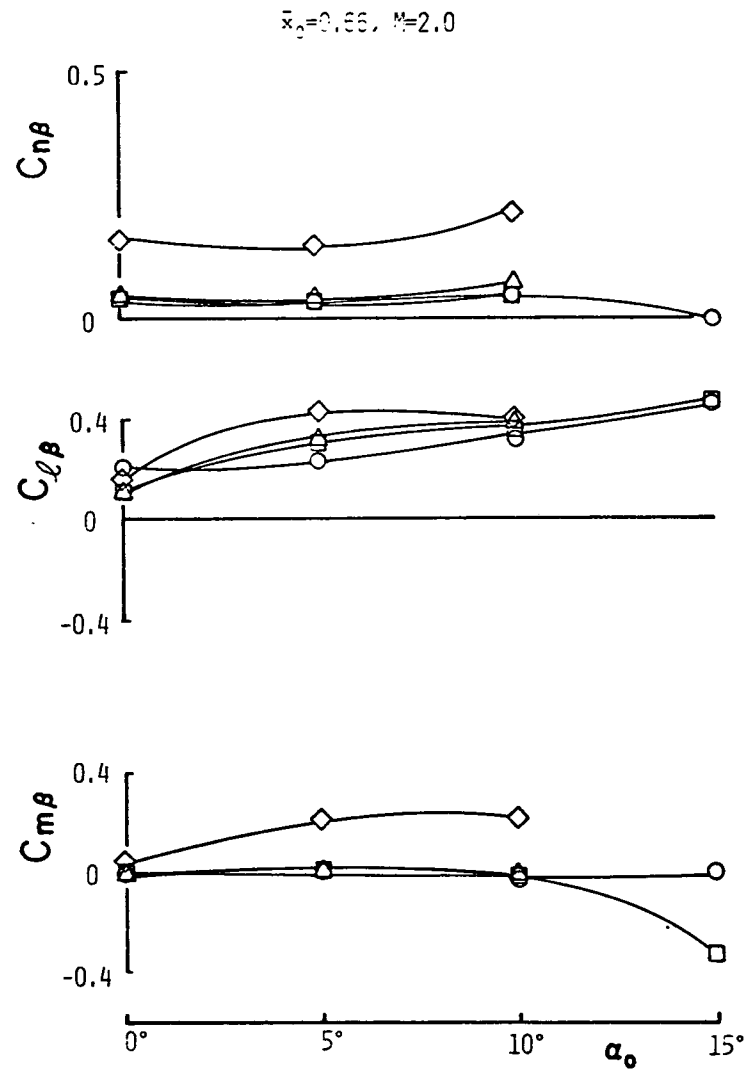
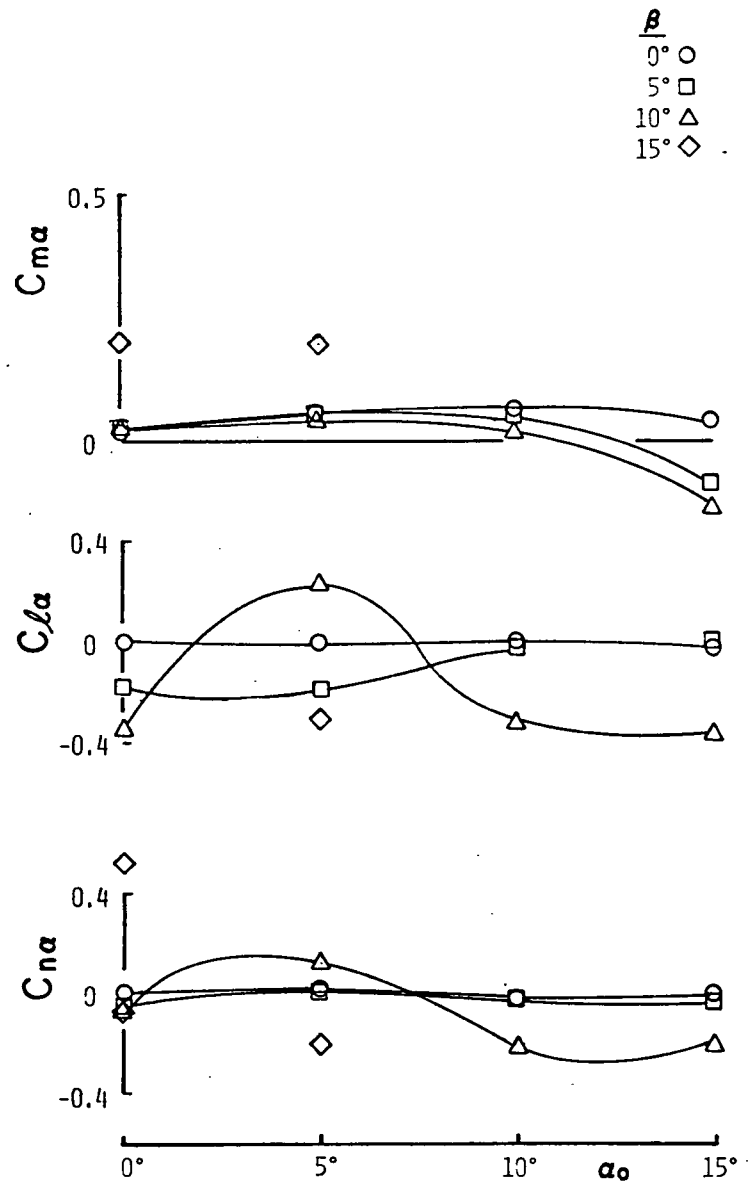


FIG. 12 · STATIC DERIVATIVES AS FUNCTION OF α_0

α

- 0° ○
- 5° □
- 10° △
- 15° ◇

$\bar{x}_0=0.55, M=2.0$

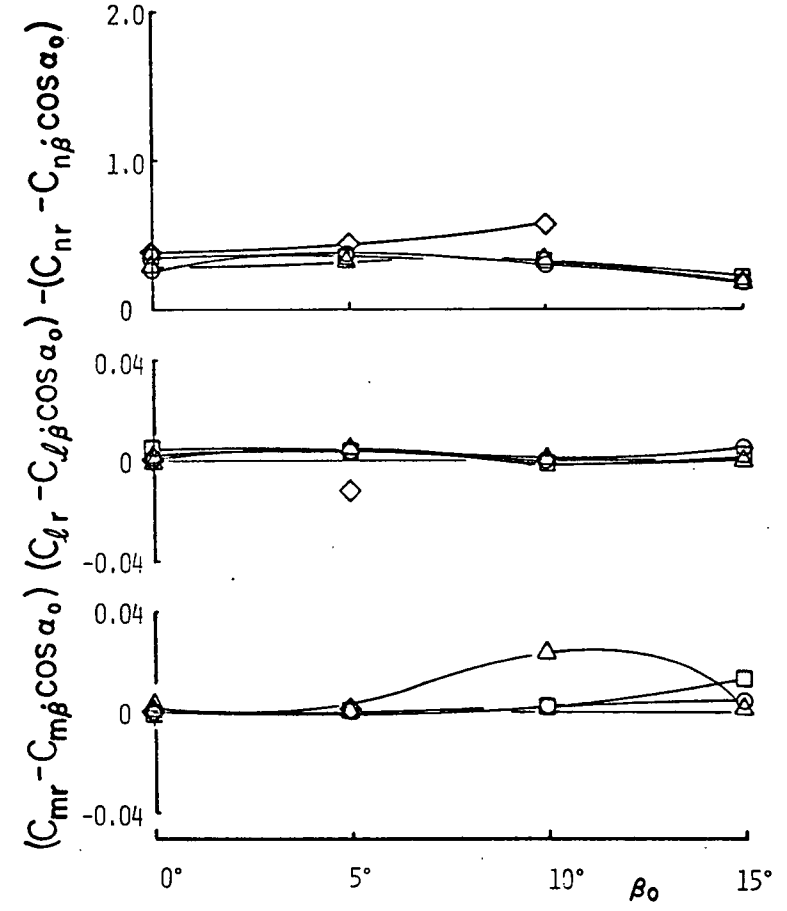
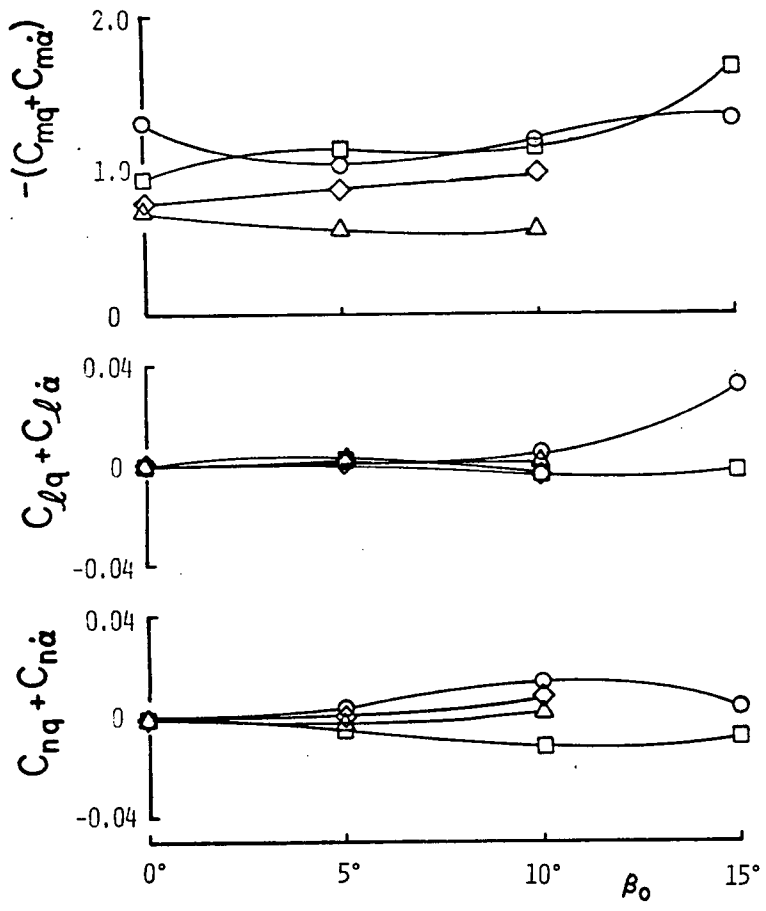


FIG. 13 DYNAMIC DERIVATIVES AS FUNCTION OF β_0

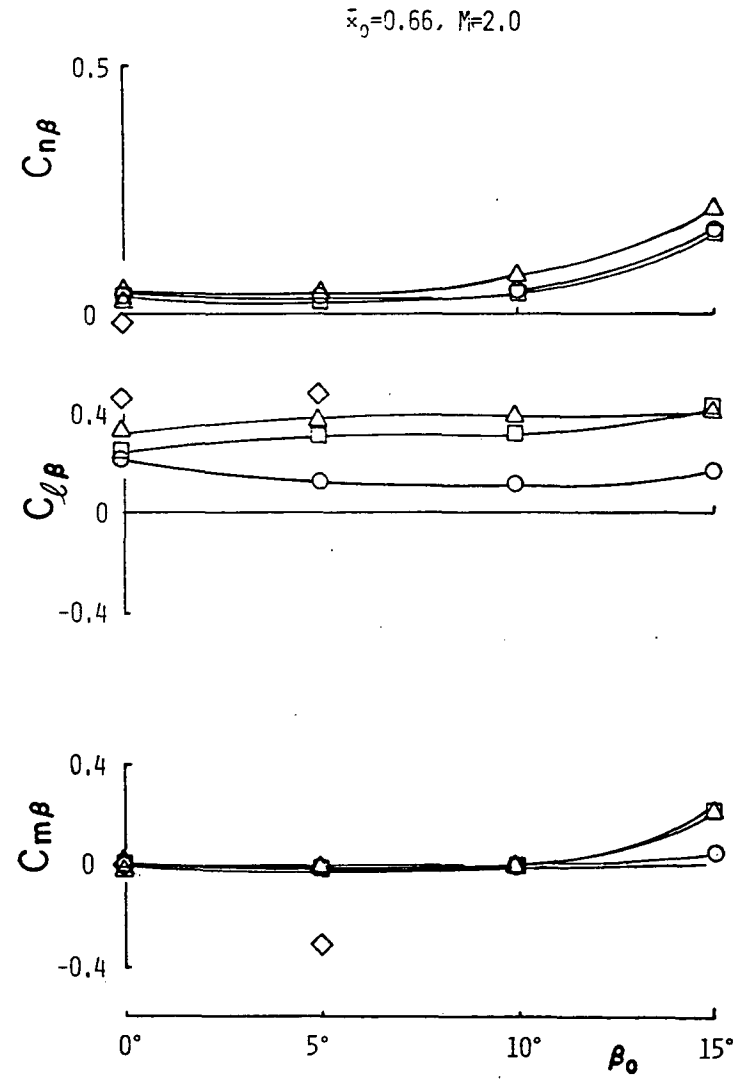
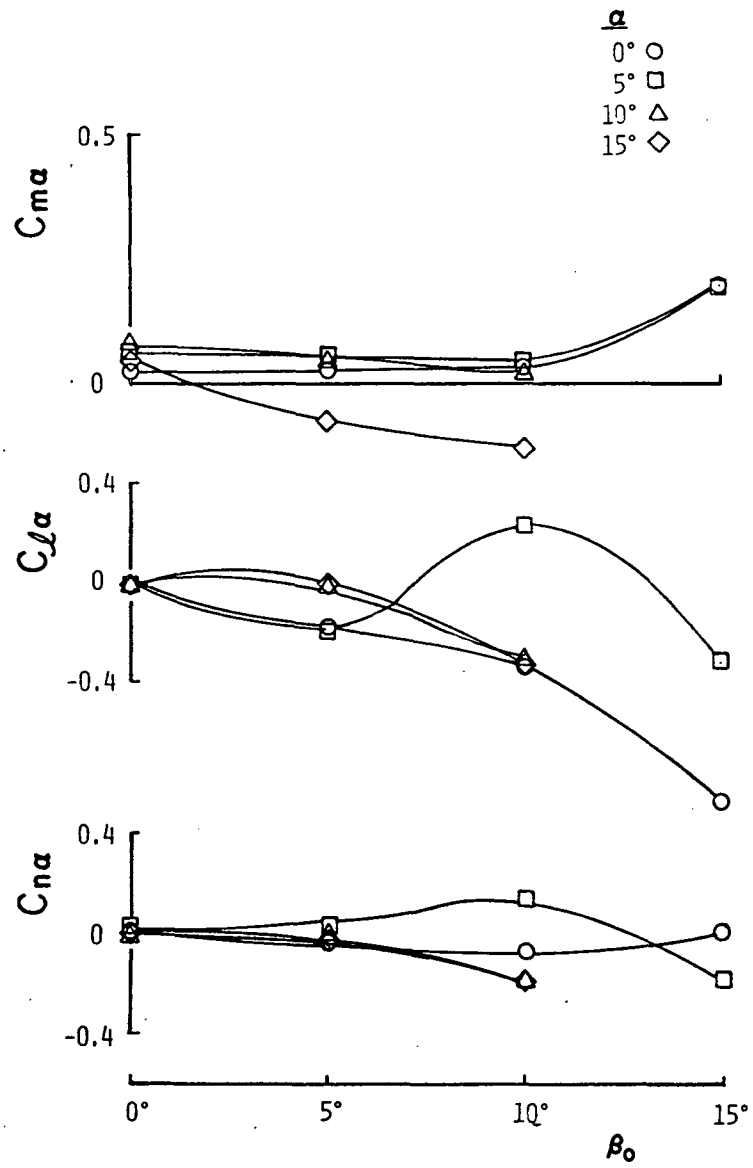


FIG. 14 STATIC DERIVATIVES AS FUNCTION OF β_0